Available online at www.sciencedirect.com

SCIENCE DIRECT®

International Journal of Thermal Sciences 45 (2006) 367–377

International Journal of Thermal Sciences

www.elsevier.com/locate/ijts

Steady filmwise condensation with suction on a finite-size horizontal flat plate embedded in a porous medium based on Brinkman and Darcy models

Shih-Chieh Wang [a], Cha'o-Kuang Chen [b,*], Yue-Tzu Yang [b]

[a] Department of Computer Application Engineering, Far East College, Tainan 744, Taiwan, ROC

[b] Department of Mechanical Engineering, National Cheng Kung University, Tainan 701, Taiwan, ROC

Received 13 May 2004; received in revised form 18 October 2004; accepted 18 October 2004

Available online 6 July 2005

Abstract

The steady filmwise condensation outside a finite-size horizontal plate covered with a thick porous medium layer is investigated numerically by boundary layer approximations and Brinkman model. The fourth-order Runge–Kutta scheme and shooting method are employed to solve numerically the nonlinear ordinary differential equation. The results are presented in terms of the dimensionless average Nusselt number $\overline{Nu}$ and the dimensionless condensate thickness $\overline{\delta_L^*}$. It is shown from the results presented that the Nusselt number increases with increasing suction parameter and it is also the function of various parameters, such as Darcy number, *Da*, Jacob number, *Ja*, Prandtl number, *Pr*, modified Rayleigh number for a porous medium, *Ra*, and permeability parameter, λ_0. It is also shown that the boundary effect plays an important role for the condensation heat transfer rate in a porous medium.

Keywords: Laminar filmwise condensation; Porous medium; Brinkman model

1. Introduction

The problem of laminar condensation on a vertical or nearly vertical wall has been subject to Nusselt's [1] four major assumptions and predicted the heat transfer rate. The laminar condensation problem has been studied by Rohsenow [2], Sparrow and Gregg [3], Chen [4], and Denny and Mills [5], etc. since 1916. Koh et al. [6,7] found that the effects of interfacial shear stress on heat transfer were small or negligible, but Nusselt numbers reduction occurred in the range of liquid-metal Prandtl numbers. Churchill [8] obtained the closed form results to the effects of the inertia and the heat capacity of the condensate, the drag of the vapor and the curvature. Méndez and Treviño [9] extensively considered the effects of both longitudinal and transversal heat conduction for a vertical flat wall, and they obtained the asymptotic and numerical solutions for the temperature and condensate film thickness profiles. Cheng [10] explored the problem of a laminar filmwise condensation along a wedge or a cone embedded in a porous medium by using Darcy model.

Jain and Bankoff [11] solved the problem of condensation along a vertical wall with constant suction velocity, and they obtained an exact solution by using a double power perturbation method. Frankel and Bankoff [12] looked into the condensation on horizontal tubes in a porous medium problem. Yang [13] solved governing equations by a series expansion method and the results importantly involved sub-cooling parameter, Prandtl number, and suction velocity parameter. Liu et al. [14] supplied a similarity solution of film condensation in a porous medium with an appropriate distribution of lateral mass flux on a body surface of arbitrary shape. Ebinuma and Liu [15] considered the Liu's special case in which the wall temperature varies with distance along the symmet-

* Corresponding author. Tel.: +886 6 2757575 ext. 62140; fax: +886 6 2342081.

E-mail address: ckchen@mail.ncku.edu.tw (C.-K. Chen).

1290-0729/$ – see front matter © 2005 Elsevier SAS. All rights reserved.
doi:10.1016/j.ijthermalsci.2004.10.008

Nomenclature

C	the Ergun constant	
C_p	specific heat at constant pressure	$\mathrm{J{\cdot}kg^{-1}{\cdot}K^{-1}}$
Da	Darcy number defined in Eq. (20)	
g	acceleration of gravity	$\mathrm{m{\cdot}sec^{-2}}$
h	convection heat transfer coefficient	$\mathrm{W{\cdot}m^{-2}{\cdot}K^{-1}}$
h_x	local convection heat transfer coefficient	$\mathrm{W{\cdot}m^{-2}{\cdot}K^{-1}}$
h_{fg}	latent heat of condensation	$\mathrm{J{\cdot}kg^{-1}}$
Ja	Jacob number defined in Eq. (20)	
k_{eff}	effective thermal conductivity	$\mathrm{W{\cdot}m^{-1}{\cdot}K}$
K	intrinsic permeability of a porous medium	$\mathrm{m^2}$
L_0	half length of a finite-size horizontal flat plate	m
$\dot{m}$	condensate mass flux defined in Eq. (15)	$\mathrm{kg{\cdot}s^{-1}}$
Nu	Nusselt number defined in Eq. (31)	
P	pressure	Pa
Pr	Prandtl number defined in Eq. (20)	
$\Re$	defined in Eq. (12)	
Ra	modified Rayleigh number defined in Eq. (20)	
Re_w	Reynolds number at surface defined in Eq. (20)	
S_w	suction parameter at surface defined in Eq. (20)	
T	temperature of condensate	K
ΔT	saturation temperature minus surface temperature	°C
u	velocity of condensate in x-direction	$\mathrm{m{\cdot}s^{-1}}$
v	velocity of condensate in y-direction	$\mathrm{m{\cdot}s^{-1}}$
v_w	suction velocity on the plate surface	$\mathrm{m{\cdot}s^{-1}}$
x	axial coordinate	m
y	transverse coordinate	m

Greek letters

α_a	apparent thermal diffusivity of a porous medium	$\mathrm{m^2{\cdot}s^{-1}}$
δ_L	local condensate thickness	m
ϕ	porosity of a porous medium	
η	dimensionless condensate thickness defined by δ_L/L_0	
Θ	parameter defined as, $= h_{fg} + C_p\Delta T/2$	$\mathrm{J{\cdot}kg^{-1}}$
λ	parameter defined as, $= \sqrt{\varepsilon/K}$	$\mathrm{m^{-1}}$
λ_0	permeability parameter defined as, $= (\varepsilon/Da)^{1/2}$	
μ_{eff}	effective viscosity of condensate in a porous medium	$\mathrm{kg{\cdot}m^{-1}{\cdot}s^{-1}}$
ρ	density of condensate	$\mathrm{kg{\cdot}m^{-3}}$
ζ_1	dimensionless condensate thickness, i.e., $\zeta_1 = \eta$	
ζ_2	gradient of dimensionless condensate thickness, i.e., $\zeta_2 = \eta'$	
$\Delta\overline{\delta_L^*}$	variation percent of average film thickness defined in Eq. (32)	
$\Delta\overline{Nu}$	variation percent of average Nusselt number defined in Eq. (30)	

Superscripts

$*$	indicates dimensionless quantity
$\overline{}$	indicates average quantity

Subscripts

0	quantity at central point of flat plane surface
a	apparent quantity
c	critical quantity or quantity at the flat surface edge
eff	effective properties
L	quantity associated with the condensate
sat	saturated properties
w	finite-size horizontal flat plane surface
x	local properties

ric body. Pop and Ingham [16] investigated the problem of flow past a sphere embedded in a porous medium based on the Brinkman model and presented a closed form solution. Based on the Darcy–Brinkman–Forchheimer model (DBF model), Al-Nimr and Alkam [17] investigated the film condensation with and without the microscopic inertia effect on a vertical plate in a porous medium. Thus, they obtained two kind of closed-form results. Char et al. [18] studied the problem of mixed convection condensate along a conducting vertical plate in a porous medium by using the DBF model and found the local heat transfer rate increased with a decrease in the Jacob number, the Peclet number, and the inertial parameter. It should be mentioned here the one side flow.

A treatment of condensation problem for horizontal flat surface has been presented by Popov [19]. Condensation under side or upper side of a horizontal or inclined surface has been investigated by several authors. Yang and Chen [20] used the concept of hydraulics of open channel flow to search the boundary condition at the edge of the plate. Yang et al. [21] considered the condensation on a finite-size horizontal wavy disk and on a plate facing upward based on the Bakhmeteff's [22] assumption used by, which is the minimum mechanical energy with respect to the boundary layer thickness at the edge of the plate. Based on the Darcy model (DM), Wang et al. [23] recently discussed the problem of boundary layer condensation along horizontal flat plane embedded in a porous medium and they got exact solutions.

The present paper studies the suction effect on the laminar film condensation on a finite-size horizontal permeable flat plate embedded in a porous medium. The objective is to consider both the Brinkman and Darcy model equations of motion for the condensate flow in the boundary layer and examine the significance of each model. The effects of several key parameters on the average Nusselt number and dimensionless film thickness have been examined.

2. Mathematical model

The two-dimensional laminar condensation on a horizontal permeable flat plate embedded in a porous medium is considered as shown in Fig. 1. The surface temperature T_w of the plate is uniform and the temperature of saturated vapor in a porous medium corresponds to the saturated temperature T_{sat}. It is assumed that porous medium is an isotropic material. It is also assumed that the flow of condensate depends on the variation in hydrostatic pressure. The porous medium layer is saturated with the condensate. We consider Stokes's flow for condensate in a porous medium layer. The momentum boundary layer is furthermore subject to a uniform suction, which removes the condensate at a constant suction velocity. Then, the condensate flows past the finite surface under the influence of gravity. In order to study the problem of film condensation about a horizontal flat plane with homogeneous porous medium layer, the Brinkman model (BM) and Darcy model (DM) are applied to both the dry vapor and liquid phases in a porous medium. Attention will be restricted to steady-state flows in this analysis and multiphase flows will not be intended.

The continuity equation for condensate forced flow through a porous medium is, if density variations are negligible:

$$\partial u_L/\partial x + \partial v_L/\partial y = 0 \tag{1}$$

where the subscript L denotes the quantity associated with the condensate; u_L and v_L are the velocity components in the x- and y-directions, respectively. The governing momentum equation for the condensate within $y \leqslant \delta_L$ under the boundary layer simplifications is given as for BM:

$$\partial^2 u_L/\partial y^2 = \phi u_L/K + \phi(\partial P/\partial x)/\mu_{\text{eff}} \tag{2a}$$

Eq. (2a) represents the Brinkman extension of Darcy model, which is considered by neglecting buoyancy force where the first term on the left-hand side of the Eq. (2a) is the Brinkman term, which accounts for the presence of a solid boundary effect. In Eq. (2a), ϕ is a porosity of a porous medium, K is a permeability of a porous medium, P is the local pressure, μ_{eff} is the effective dynamic viscosity of the condensate in a porous medium. If the permeability of the porous medium is very high, it may be impossible to neglect the viscous forces in setting up the momentum equation. Based on the Darcy model (DM), it must be noted that the effects of viscosity are being ignored, we have:

$$u_L = K(-\partial P/\partial x)/\mu_L \tag{2b}$$

where μ_L is the dynamic viscosity of the condensate. In addition, the equation of momentum at y-direction will be given by:

$$0 = -\partial P/\partial y - \rho_L g \tag{3}$$

if the buoyancy forces are considered. The energy equation will assume that the condensate and the particulate material are in thermodynamic equilibrium, so that it is given by:

$$u_L \frac{\partial T_L}{\partial x} + v_L \frac{\partial T_L}{\partial y} = \alpha_a \frac{\partial^2 T_L}{\partial y^2} \tag{4}$$

In Eqs. (3) and (4), g is the gravitational acceleration, ρ_L is the density of condensate, α_a is the apparent thermal diffusivity of the condensate in a porous medium. If the porous particles are spherical, the permeability of a porous medium K is based on the expression determined experimentally by Ergun [24]:

$$K = \frac{\phi^3 d_p^2}{C_E(1-\phi)^2}$$

where the d_p is a mean diameter of solid particle and the symbol C_E is the Ergun constant depending on the matrix of a porous medium. Furthermore, it is assumed that the effects of non-condensable gas, shear stress at the interface between the condensate and the pure vapor, surface–tension–driven convection in the porous–fluid system, and capillary suction in a porous layer can be neglected. Eqs. (1)–(4) are subjected to the boundary conditions presented as follows:

at the plate surface ($y = 0$)

$$T_L = T_w, \qquad v_L = -v_w$$
$$(u_L = 0,\ \text{only for BM}) \tag{5}$$

at the vapor–liquid interface ($y = \delta_L(x)$)

$$T_L = T_{\text{sat}}, \qquad P = P_{\text{sat}}, \qquad \partial u_L/\partial y = 0 \tag{6}$$

where T_w is the temperature of flat surface, which is constant; T_{sat} is the saturated temperature of a vapor; P_{sat} is the saturated pressure corresponding to the saturated temperature T_{sat}; $\delta_L(x)$ is the local condensate thickness which is to be determined.

Integrating Eq. (3) and imposing the boundary condition given by Eq. (6), we can obtain the static pressure term as follow:

$$P = P_{\text{sat}} + \rho_L g(\delta_L - y) \tag{7}$$

Solving for u_L and substituting Eq. (7) into Eqs. (2a) and (2b), and integrating Eqs. (2a) and (2b) subject to appropriate boundary conditions given by Eqs. (5) and (6), gives the x-directional velocity profiles:

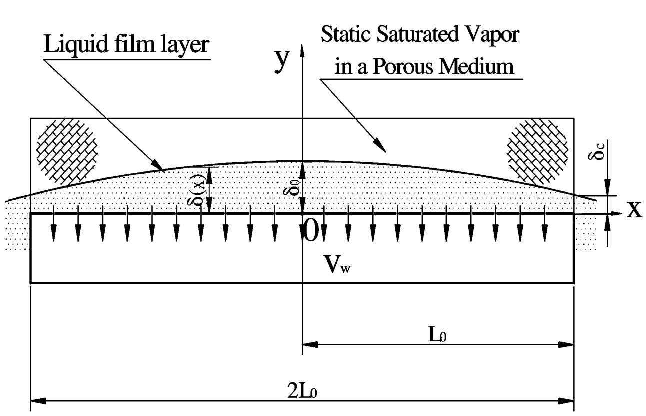

Fig. 1. Physical model and coordinate system.

$$u_L = -\frac{\rho_L g K}{\mu_{\text{eff}}}\left\{1 - \frac{\text{Cosh}[\lambda(\delta_L - y)]}{\text{Cosh}(\lambda\delta_L)}\right\}\delta_L' \quad \text{for BM} \tag{8a}$$

$$u_L = -(\rho_L g K/\mu_L)\delta_L' \quad \text{for DM} \tag{8b}$$

where $\lambda = \sqrt{\phi/K}$ is a constant for a specified porous medium layer, and prime denotes differentiation with respect to x, i.e. $\delta_L' = \mathrm{d}\delta_L/\mathrm{d}x$, $\delta_L'' = \mathrm{d}^2\delta_L/\mathrm{d}x^2$. Using the above results, Eqs. (8a) and (8b), and the boundary condition given by Eq. (5) and integrating Eq. (1), we can obtain the velocity profiles in the y-direction as:

$$\begin{aligned} v_L = \left(\frac{\rho_L g K}{\lambda\mu_{\text{eff}}}\right)\bigl\{&\delta_L''\bigl[\text{Sinh}(\lambda y) \\ &+ \bigl(1 - \text{Cosh}(\lambda y)\bigr)\cdot\text{Tanh}(\lambda\delta_L) - \lambda\cdot y\bigr] \\ &- 2\lambda\delta_L'^2\cdot\text{Sech}^2(\lambda\delta_L)\cdot\text{Sinh}^2(\lambda y/2)\bigr\} - v_w \end{aligned}$$
$$\text{for BM} \tag{9a}$$

$$v_L = (\rho_L g K\delta_L''/\mu_L)y - v_w \quad \text{for DM} \tag{9b}$$

Both the first law of thermodynamics and mass conservation equation are considered to be coupled in the governing equations. Hence, the steady balance of thermal energy at both condensate in a porous medium and plate surface with suction effect accomplished by the following equation [23]:

$$k_a\frac{\partial T_L}{\partial y}\bigg|_{y=0} = \rho_L v_w(h_{\text{fg}} + C_p\Delta T) + \frac{\mathrm{d}}{\mathrm{d}x}\left[\int_0^{\delta_L(x)}\rho_L u_L\bigl[h_{\text{fg}} + C_p(T_s - T_L)\bigr]\,\mathrm{d}y\right] \tag{10}$$

where C_p is the specific heat at constant pressure of the condensate fluid, h_{fg} is a latent heat of condensate, ΔT is the reference temperature difference between the saturation temperature of vapor in a porous layer and plate surface temperature. The apparent thermal conductivity, k_a, that occurs in Eq. (10) is a result of conduction in the porous medium matrix and in the fluid including the effect of thermal dispersion, and has to be usually measured experimentally. Otherwise, the quantity of apparent thermal diffusivity, α_a, that occurs in the energy equation (4) is equal to $(k_a/\rho_L C_p)$. It is assumed that the suction velocity v_w is constant along the horizontal plate. Because the condensate thickness $\delta_L(x)$ is relatively small compared to the half-length L_0 of the plate, the convective term is then ignored from the energy equation (4). The laminar temperature profile implies that

$$T_L = y\Delta T/\delta_L(x) + T_w \tag{11}$$

Substituting Eqs. (11), (8a) and (8b) into Eq. (10), one gets:

$$\begin{aligned} &\delta_L\frac{\mathrm{d}}{\mathrm{d}x}\bigl[\delta_L\delta_L'(1-\Re)\bigr] \\ &\quad = \frac{-k_a\mu_{\text{eff}}\Delta T}{\rho_L^2 K g(h_{\text{fg}} + C_P\Delta T/2)} + \frac{v_w\mu_{\text{eff}}(h_{\text{fg}} + C_P\Delta T)\delta_L}{\rho_L K g(h_{\text{fg}} + C_P\Delta T/2)} \end{aligned}$$
$$\text{for BM} \tag{12a}$$

where

$$\Re = \frac{(h_{\text{fg}} + C_P\Delta T)\text{Tanh}(\lambda\delta_L)}{\lambda\delta_L(h_{\text{fg}} + C_P\Delta T/2)} + \frac{C_P\Delta T[\text{Sech}(\lambda\delta_L) - 1]}{\lambda^2\delta_L^2(h_{\text{fg}} + C_P\Delta T/2)}$$

$$\delta_L\frac{\mathrm{d}}{\mathrm{d}x}(\delta_L\delta_L') = \frac{-k_a\mu_L\Delta T}{\rho_L^2 K g(h_{\text{fg}} + C_P\Delta T/2)} + \frac{v_w\mu_L(h_{\text{fg}} + C_P\Delta T)\delta_L}{\rho_L K g(h_{\text{fg}} + C_P\Delta T/2)} \quad \text{for DM} \tag{12b}$$

The corresponding boundary condition is expressed as

$$\delta_L' = 0 \quad \text{at } x = 0 \tag{13}$$

In fact, we cannot solve Eqs. (12a) and (12b) with their boundary condition (13) yet. In accordance with a minimum mechanical energy principle, presented by Bakhmeteff [22] about the concept of hydraulics of open channel flow, we need to find a new boundary condition to solve Eqs. (12a) and (12b). Referring to Bakhmeteff's theory, the relation equation can be defined as:

$$\frac{\partial}{\partial\delta_c}\left(\int_0^{\delta_L(x)}\left(\frac{u_L^2}{2} + gy + \frac{P}{\rho_L}\right)\rho_L u_L\,\mathrm{d}y\right)\bigg|_{\dot{m}=\dot{m}_c} = 0 \tag{14}$$

where δ_c is a condensate thickness at the edge of plate, but it is still unknown, and $\dot{m}_c$ is the critical value of mass flow rate out of the plate edge. Supposing that the velocity u_L given by Eqs. (8a) and (8b) is very larger the velocity v_L expressed by Eqs. (9a) and (9b), the local condensate mass flow rate should be expressed as:

$$\dot{m}_x = \int_0^{\delta_L(x)}\rho_L u_L\,\mathrm{d}y \tag{15}$$

By substituting Eqs. (8a) and (8b) into Eq. (15), we can easily obtain the following equations:

$$\dot{m}_x = -\bigl[\rho_L^2 g K/\lambda\mu_{\text{eff}}\bigr]\bigl(\lambda\delta_L - \text{Tanh}(\lambda\delta_L)\bigr)\delta_L'$$
$$\text{for BM} \tag{16a}$$

$$\dot{m}_x = -\bigl[\rho_L^2 g K/\mu_L\bigr]\delta_L\delta_L' \quad \text{for DM} \tag{16b}$$

The critical values of mass flow rate $\dot{m}_c$ at $x = L_0$, are given by:

$$\dot{m}_c = \bigl[\rho_L^2 g K/\lambda\mu_{\text{eff}}\bigr]\bigl[\lambda\delta_c - \text{Tanh}(\lambda\delta_c)\bigr]\delta_L'\big|_{x=L_0}$$
$$\text{for BM} \tag{17a}$$

$$\dot{m}_c = -\bigl[\rho_L^2 g K/\mu_L\bigr]\delta_c\delta_L'\big|_{x=L_0} \quad \text{for DM} \tag{17b}$$

It is assumed that it is not to necessary for the edge thickness δ_c to become zero at any specified conditions. Referring to Eq. (14) subject to boundary conditions (13), (17a) and (17b), we can obtain the following relation:

$$\begin{aligned} \dot{m}_c^2 = \frac{4g\rho_L^2}{\lambda^3\text{Sinh}(\lambda\delta_c)}\bigl\{&\bigl[\lambda\delta_c\text{Cosh}(\lambda\delta_c) - \text{Sinh}(\lambda\delta_c)\bigr]^4 \\ &\times\bigl[\lambda\delta_c\bigl[6\lambda\delta_c\text{Cosh}(\lambda\delta_c) + \text{Sinh}(3\lambda\delta_c)\bigr] \\ &- 9\text{Cosh}(\lambda\delta_c)\text{Sinh}^2(\lambda\delta_c)\bigr]^{-1}\bigr\} \quad \text{for BM} \end{aligned} \tag{18a}$$

$$\dot{m}_c^2 = \rho_L^2 g\delta_c^3 \quad \text{for DM} \tag{18b}$$

Combining Eqs. (17a) and (18a) yields the new boundary condition for BM:

$$\begin{aligned}\delta_L'\big|_{x=L_0} &= 2\mu_{\text{eff}}\text{Cosh}(\lambda\delta_c)\big[\text{Sinh}(\lambda\delta_c)-\lambda\delta_c\text{Cosh}(\lambda\delta_c)\big]\\ &\quad\times\big[(\lambda g)^{1/2}\rho_L K\big\{\lambda\delta_c\text{Sinh}(\lambda\delta_c)\text{Sinh}(3\lambda\delta_c)\\ &\quad+3\text{Cosh}(\lambda\delta_c)\text{Sinh}(\lambda\delta_c)\big[2\lambda\delta_c-3\text{Sinh}^2(\lambda\delta_c)\big]\big\}^{1/2}\big]^{-1}\\ &\quad\text{for BM} \qquad (19a)\end{aligned}$$

and coupling Eqs. (17b) and (18b) provides the new boundary condition for DM:

$$\delta_L'\big|_{x=L_0} = -\big[\mu_L^2\delta_c/\big(\rho_L^2 gK^2\big)\big]^{1/2} \quad \text{for DM} \qquad (19b)$$

To simplify this analysis, the value of μ_L is assumed to be equal to μ_{eff} [25] and the following non-dimensional variables allow the preceding equations to be transformed into a non-dimensional form:

$$\begin{aligned}&x^*=\frac{x}{L_0},\qquad \eta=\frac{\delta_L}{L_0},\qquad \delta_0^*=\frac{\delta_0}{L_0},\qquad \delta_c^*=\frac{\delta_c}{L_0}\\ &Da=\frac{K}{L_0^2},\qquad Ja=\frac{C_p\Delta T}{\Theta}\\ &Pr=\frac{\mu_{\text{eff}}C_p}{k_a},\qquad Ra=\frac{\rho_L^2 gPr L_0^3}{\mu_{\text{eff}}^2}\\ &S_w=\frac{Pr\,Re_w}{Ja}(1+Ja/2),\qquad Re_w=\frac{\rho_L v_w L_0}{\mu_{\text{eff}}}\\ &u^*=\frac{u_L}{(gL_0)^{1/2}},\qquad v^*=\frac{v_L}{(gL_0)^{1/2}}\\ &\lambda_0=(\phi/Da)^{1/2} \qquad (20)\end{aligned}$$

where $\Theta = h_{\text{fg}} + C_p\Delta T/2$. Here δ_0 is the condensate thickness at the central point of a plate, Da is the Darcy number, Ja is the Jacob number, Pr is the Prandtl number, Ra is the Darcy-modified Rayleigh number for a porous medium, Re_w is the Reynolds number for suction along the plate surface, S_w is the suction parameter, u^* and v^* are the dimensionless Darcian–Brinkman velocity components in the x- and y-directions, respectively, and λ_0 is called permeability parameter. The permeability parameter λ_0 plays a very important role in this analysis. In terms of these new variables, the new boundary conditions in Eqs. (19a) and (19b) become in non-dimensional form:

$$\begin{aligned}\left(\frac{\mathrm{d}\eta}{\mathrm{d}x^*}\right)\bigg|_{x^*=1} &= 2Pr^{1/2}Ra^{-1/2}\lambda_0^{-1/2}\text{Cosh}\big(\lambda_0\delta_c^*\big)\\ &\quad\times\big[\text{Sinh}\big(\lambda_0\delta_c^*\big)-\lambda_0\delta_c^*\text{Cosh}\big(\lambda_0\delta_c^*\big)\big]\\ &\quad\times\big[Da\big\{\lambda_0\delta_c^*\text{Sinh}\big(\lambda_0\delta_c^*\big)\text{Sinh}\big(3\lambda_0\delta_c^*\big)\\ &\quad+3\text{Cosh}\big(\lambda_0\delta_c^*\big)\text{Sinh}\big(\lambda_0\delta_c^*\big)\\ &\quad\times\big[2\lambda_0\delta_c^*-3\text{Sinh}^2\big(\lambda_0\delta_c^*\big)\big]\big\}^{1/2}\big]^{-1} \quad \text{for BM} \qquad (21a)\end{aligned}$$

$$\left(\frac{\mathrm{d}\eta}{\mathrm{d}x^*}\right)\bigg|_{x^*=1} = -\big[Pr\,\delta_c^*/\big(Da^2 Ra\big)\big]^{1/2} \quad \text{for DM} \qquad (21b)$$

where δ_c^* is the non-dimensional condensate thickness at the edge of plate, i.e. at $x^*=1$, and is still unknown. By using Eq. (20), the Eqs. (12a) and (12b) with their boundary condition (13) can transform to:

$$\eta\frac{\mathrm{d}}{\mathrm{d}x^*}\left[\eta(1-\Re^*)\frac{\mathrm{d}\eta}{\mathrm{d}x^*}\right] = \left(\frac{Ja}{Da\,Ra}\right)(S_w\eta-1) \quad \text{for BM} \qquad (22a)$$

$$\eta\frac{\mathrm{d}}{\mathrm{d}x^*}\left[\eta\frac{\mathrm{d}\eta}{\mathrm{d}x^*}\right] = \left(\frac{Ja}{Da\,Ra}\right)(S_w\eta-1) \quad \text{for DM} \qquad (22b)$$

$$\frac{\mathrm{d}\eta}{\mathrm{d}x^*} = 0 \quad \text{at } x^*=0 \qquad (23)$$

In Eq. (22a), the symbol $\Re^*$ is a function of x^* only and is defined as

$$\begin{aligned}\Re^* &= (1+Ja/2)\text{Tanh}(\lambda_0\eta)/(\lambda_0\eta)\\ &\quad+Ja\big[\text{Sech}(\lambda_0\eta)-1\big]/(\lambda_0\eta)^2 \qquad (24)\end{aligned}$$

From Eq. (20), the non-dimensional velocity of suction can be also calculated and is given by the following expression:

$$v_w^* = S_w/\big[(Pr\,Ra)^{1/2}(1/Ja+0.5)\big] \qquad (25)$$

Substituting Eqs. (20) and (25) into Eqs. (8a) and (8b) gives the following non-dimensional Darcian–Brinkman velocity components in the x- and y-directions,

$$u^* = \left(\frac{Da\,Ra}{Pr^{1/2}}\right)\left\{\frac{\text{Cosh}[\lambda_0(\eta-y^*)]}{\text{Cosh}(\lambda_0\eta)}-1\right\}\eta' \qquad (26)$$

$$\begin{aligned}v^* &= \left(\frac{Da\,Ra}{\lambda_0 Pr^{1/2}}\right)\big\{\eta''\big[\text{Sinh}(\lambda_0 y^*)-\lambda_0 y^*\\ &\quad+\big[1-\text{Cosh}(\lambda_0 y^*)\big]\text{Tanh}(\lambda_0\eta)\big]\\ &\quad-2\lambda_0\eta'^2\text{Sech}^2(\lambda_0\eta)\text{Sinh}^2(\lambda_0 y^*/2)\big\}\\ &\quad-\frac{S_w}{(1/Ja+0.5)(Pr\,Ra)^{1/2}} \qquad (27)\end{aligned}$$

One of the most interesting physical quantity is the local Nusselt number, Nu_x, which can be defined as

$$Nu_x = L_0 h_x/k = 1/\eta(x^*) \qquad (28)$$

where h_x is the local heat transfer coefficient. The average heat transfer coefficient, $\bar{h}$, can be expressed as:

$$\begin{aligned}\bar{h} &= \int_0^{L_0}(h_x/L_0)\,\mathrm{d}x = -\int_0^{L_0}\frac{k_a}{L_0\Delta T}\left(\frac{\partial T}{\partial y}\right)_w\mathrm{d}x\\ &= \frac{k_a}{L_0}\int_0^1\frac{1}{\eta(x^*)}\,\mathrm{d}x^* \qquad (29)\end{aligned}$$

In addition, the average Nusselt number, $\overline{Nu}$, is given by:

$$\overline{Nu} = \bar{h}\Delta T/(k_a\Delta T/L_0) = \int_0^1(1/\eta)\,\mathrm{d}x^* \qquad (30)$$

Furthermore, the variation of average Nusselt number, $\Delta\overline{Nu}$, is given by the following relation:

$$\Delta\overline{Nu} = \left[\left(\overline{Nu} - \overline{Nu}\big|_{S_w=0}\right)/\overline{Nu}\big|_{S_w=0}\right] \times 100\% \tag{31}$$

The variation of average non-dimensional film thickness, $\Delta\overline{\delta_L^*}$, can be defined as

$$\Delta\overline{\delta_L^*} = \left[\left(\overline{\delta_L^*} - \overline{\delta_L^*}\big|_{S_w=0}\right)/\overline{\delta_L^*}\big|_{S_w=0}\right] \times 100\% \tag{32}$$

In order to discuss the variation of the flow and heat transfer quantities with suction or without suction, we define Eqs. (31) and (32). In addition, the average non-dimensional film thickness, $\overline{\delta_L^*}$, in Eq. (32) will be represented as:

$$\overline{\delta_L^*} = \int_0^{L_0} \left(\delta_L/L_0^2\right) \mathrm{d}x = \int_0^1 \eta(x^*)\,\mathrm{d}x^* \tag{33}$$

We take the value of suction velocity v_w be zero only where we consider the Darcy flow model. Then, the solutions of Eq. (22b) are obtained by using the Newton–Raphson scheme (see Appendix A). Eqs. (22a) and (22b) with the boundary conditions (21a), (21b) and (23), respectively, are solved numerically using the fourth-order Runge–Kutta scheme and shooting method [26,27] to obtain the non-dimensional condensate profiles. Eqs. (22a) and (22b) are rewritten as the following three, first-order ordinary differential equations,

$$\zeta_1' = \zeta_2 = \eta' \quad \text{for DM and BM} \tag{34}$$

$$\begin{aligned}
\zeta_2' = \eta'' = {} & 2Ja\,\lambda_0^2(\zeta_1 S_w - 1) \\
& \times \Big[Da\,Ra\big\{2Ja\big[\mathrm{Sech}(\zeta_1\lambda_0) - 1\big] \\
& - \zeta_1\lambda_0\big[2\zeta_1\lambda_0 - (2+Ja)\mathrm{Tanh}(\zeta_1\lambda_0)\big]\big\}\Big]^{-1} \\
& + \zeta_2^2\big\{2Ja\big[\mathrm{Sech}(\zeta_1\lambda_0) - 1\big] + \zeta_1\lambda_0\mathrm{Sech}(\zeta_1\lambda_0) \\
& \times \big[\zeta_1\lambda_0\mathrm{Sech}(\zeta_1\lambda_0)\big(\mathrm{Cosh}(2\zeta_1\lambda_0) - 1 - Ja\big) \\
& + 2Ja\,\mathrm{Tanh}(\zeta_1\lambda_0)\big]\big\} \\
& \times \big[\zeta_1\big\{2Ja\big[\mathrm{Sech}(\zeta_1\lambda_0) - 1\big] \\
& - \zeta_1\lambda_0\big[2\zeta_1\lambda_0 - (2+Ja)\mathrm{Tanh}(\zeta_1\lambda_0)\big]\big\}\big]^{-1}
\end{aligned}$$

$$\text{for BM} \tag{35a}$$

$$\zeta_2' = \eta'' = \frac{Ja(\zeta_1 S_w - 1)}{Da\,Ra\,\zeta_1^2} - \frac{\zeta_2^2}{\zeta_1} \quad \text{for DM} \tag{35b}$$

subject to $\zeta_2(0) = 0$, where we have defined $\zeta_1 = \eta$ and $\zeta_2 = \eta'$. In the first integration of Eq. (34) we have to guess the unknown initial value, say, $0 < \eta(0) = \delta_0^* \leqslant 1$. The uniform step size of $\Delta x^* = 1.0 \times 10^{-5}$ is chosen and the computation converge is $|\mathrm{ERR}| \leqslant 10^{-13}$, where ERR is the corresponding value of the absolute error in the boundary conditions between Eqs. (35) and (36) at $x^* = 1$. At $x^* = 1$, we have to check if the remaining boundary conditions are satisfied:

$$\begin{aligned}
\zeta_2(1) = {} & 2Pr^{1/2}\mathrm{Cosh}(\lambda_0\zeta_1)\big[\mathrm{Sinh}(\lambda\zeta_1) - \lambda\zeta_1\mathrm{Cosh}(\lambda\zeta_1)\big] \\
& \times \Big[Da\Big\{Ra\,\lambda_0\big\{\lambda_0\zeta_1\mathrm{Sinh}(\lambda_0\zeta_1)\big[6\lambda_0\zeta_1\mathrm{Cosh}(\lambda_0\zeta_1) \\
& + \mathrm{Sinh}(3\lambda_0\zeta_1)\big] \\
& - 9\mathrm{Cosh}(\lambda_0\zeta_1)\mathrm{Sinh}^3(\lambda_0\zeta_1)\big\}\Big\}^{1/2}\Big]^{-1}
\end{aligned}$$

$$\text{for BM} \tag{36a}$$

$$\zeta_2(1) = -\left[Pr\zeta_1(1)/\left(Da^2Ra\right)\right]^{1/2} \quad \text{for DM} \tag{36b}$$

Eqs. (36a) and (36b) have to be satisfied with desired accuracy $|\mathrm{ERR}| \leqslant 10^{-13}$, i.e., $|\zeta(1)_{\text{from Eq. (35)}} - \zeta(1)_{\text{from Eq. (36)}}| \leqslant 10^{-13}$.

3. Results and discussion

Based on the numerical results obtained, it may be noted that how the δ_0^* solutions using the Newton–Raphson scheme fits into the δ_0^* solutions obtained using the Runge–Kutta scheme for $Ja = 0.15$, $Ra = 10^4$, and $S_w = 0$, as presented Table 1. It can be estimated that the relatively maximum error is lower than 0.02% between the values of $\overline{Nu}$ by the Newton–Raphson scheme and the Runge–Kutta scheme, respectively.

In the present work, Fig. 2 shows the variation of the dimensionless thickness, η, of condensate along the surface of a horizontal flat plate. It is seen that at fixed values of Da, Ja, Ra, and S_w, the value of $\eta(x^* = 0)$ decreases as Pr number increases. In addition, the smaller value of $\eta(x^* = 0)$ indicates that the relative condensate film central thickness, δ_0, to the plate length, L_0, is very thin. Furthermore, we notice that with the increase of Da number (i.e., the higher permeability of a porous medium), the film profiles are nearly a straight line. Especially, the fact is mostly remarkable for liquid metal materials condensed in a porous medium. It is also clear that, if the Pr number increases, the variation of film thickness strictly increases. This is mainly due to the

Table 1
Comparisons of solutions by Newton–Raphson scheme and solutions by Runge–Kutta scheme for $Ja = 0.15$, $Ra = 10^4$, and $S_w = 0$ by using the Darcy model

$Ja = 0.15$, $Ra = 10^4$	Solutions by Newton–Raphson scheme			Solutions by Runge–Kutta scheme		
	δ_0^*	δ_c^*	$\overline{Nu}$	δ_0^*	δ_c^*	$\overline{Nu}$
$Da = 0.01$, $Pr = 7$	0.121635	0.033546	10.83748	0.121635	0.033498	10.83966
$Da = 0.1$, $Pr = 7$	0.066396	0.045055	16.86843	0.066396	0.045049	16.86914
$Da = 0.01$, $Pr = 100$	0.119525	0.014653	11.82492	0.119524	0.014539	11.83199
$Da = 0.1$, $Pr = 100$	0.057736	0.022042	21.81584	0.057736	0.022027	21.81868
$Da = 0.01$ $Pr = 0.02$	0.180946	0.155755	5.795467	0.180946	0.155750	5.795547
$Da = 0.1$, $Pr = 0.02$	0.164328	0.161519	6.120126	0.164330	0.161520	6.120209

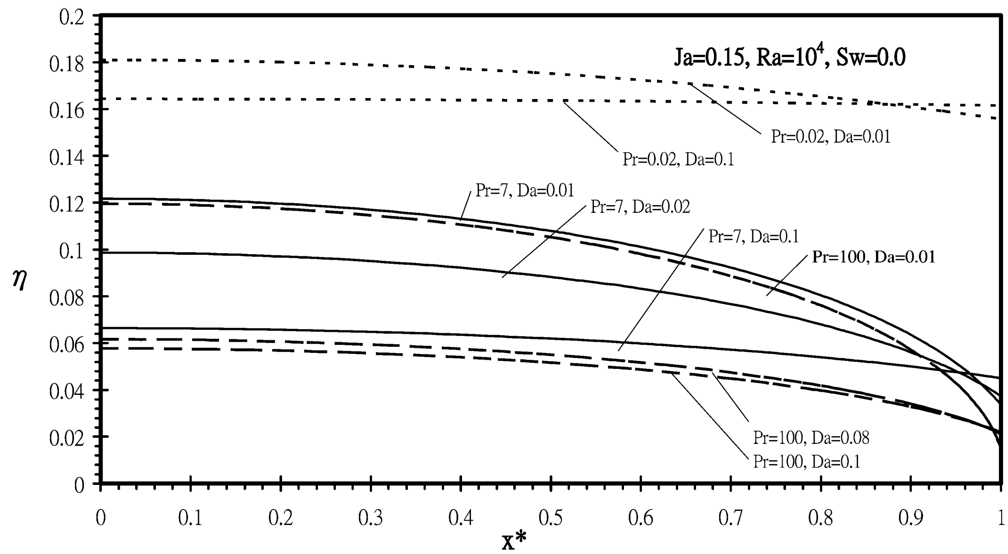

Fig. 2. Variation of the non-dimensional thickness η with dimensionless position x^* at different values of Da and Pr for $Ja = 0.15$, $Ra = 10^4$ and $S_w = 0$ by using DM.

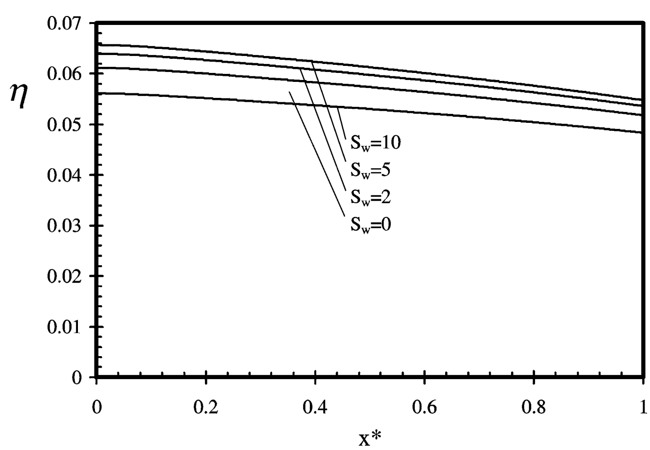

Fig. 3. Variation of the non-dimensional film profiles at different values of suction parameter S_w for $Da = 0.01$, $Ja = 0.1$, $Pr = 7$, $Ra = 2 \times 10^5$ and $\lambda_0 = 8$ based on Brinkman model (BM).

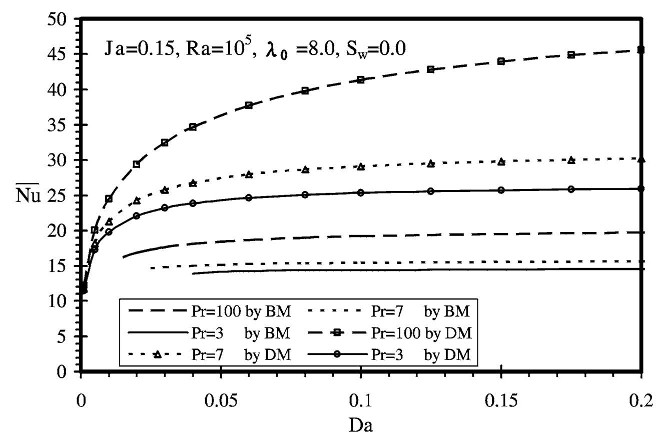

Fig. 4. Variation of $\overline{Nu}$ with Da at different values of Pr for $Ja = 0.15$, $Ra = 1 \times 10^5$, $\lambda_0 = 8$ and $S_w = 0$.

presence of relatively viscous condensation fluid motion that decreases along the plate surface.

It is apparent from Fig. 3 that the larger value of suction parameter S_w, the lower value of central dimensionless film thickness $\eta(x^* = 0)$ is obtained for fixed values of Da, Ja, Pr, Ra, and λ_0. Based on Brinkman model (BM), the variation of value of local η along horizontal plate is small. Otherwise, it reveals that the viscous effect in the condensate boundary layer gets the thicker film thickness at edge of plate and the lower variation of local slope, i.e. $\eta'(x^*)$.

The physical significance of the average Nusselt number given by Eq. (30) is a measure of the average rate of heat convection in comparison with the average rate of heat conduction across the fluid layer. A larger value of $\overline{Nu}$ implies enhanced heat transfer rate by convection and the higher heat transfer rates lead to higher condensation rates allowing the use of smaller condensers. Fig. 4 illustrates the Prandtl number effect on the average heat transfer rate, $\overline{Nu}$, vs. Darcy number, Da, at $Ja = 0.15$, $Ra = 1 \times 10^5$, $\lambda_0 = 8$ and $S_w = 0$, i.e. without suction. It is found that the value of $\overline{Nu}$ increases with the increase of Da and Pr. It is obvious that the lower Da value would bring little variation of $\overline{Nu}$ for various $Pr \geqslant 3$, since the condensate in a lower permeability porous cannot penetrate through the porous medium rapidly. Besides, under fixed values of Ja, Pr, Ra, S_w and λ_0, the value of $\overline{Nu}$ increases very slowly as Da is larger than 0.05 when we use Brinkman model to predict it. But the prediction of $\overline{Nu}$ by Darcy model is not satisfactory for the case of the liquid of higher Pr number (i.e. $Pr \geqslant 100$). Thus, it can be seen that the non-slip condition plays an important role. The higher value of λ_0 leads to values of $\overline{Nu}$ which are very close using both BM and DM models as shown in Fig. 5. This is due to the higher porosity that occurs to the shear force of condensate relatively decreasing. For liquid metal ($Pr = 0.0249$), the variation of $\overline{Nu}$ is very smaller when $Da \geqslant 0.04$ than it is $Da < 0.04$, i.e. the $\overline{Nu}$ is almost

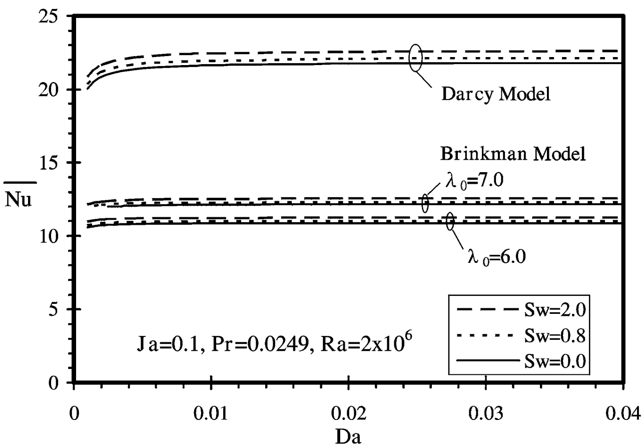

Fig. 5. Variation of the average Nusselt number, $\overline{Nu}$, with Darcy number, Da, at different values of λ_0 and S_w for $Ja = 0.1$, $Pr = 0.0249$, and $Ra = 2 \times 10^6$.

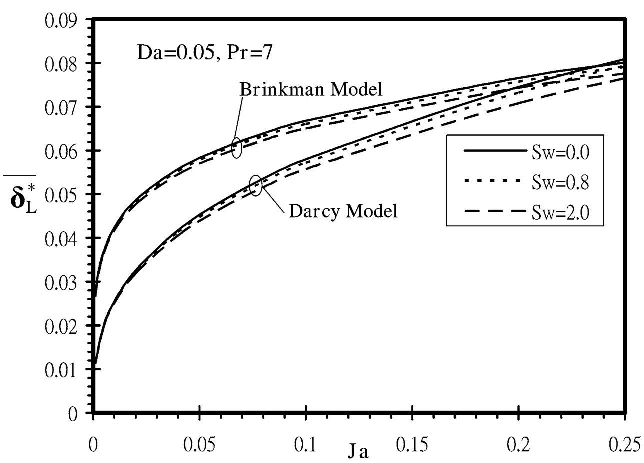

Fig. 6. Variation of the average condensate thickness, $\overline{\delta_L^*}$, with Jacob number, Ja, at different values of S_w and Ra for $Da = 5 \times 10^{-2}$, and $Pr = 7$.

a constant as $Da \geqslant 0.04$. It is due to the heat conduction mechanism plays the leading role in condensation; the momentum diffusion is much lower than the energy diffusion. Nevertheless, the effect of permeability of a porous medium is negligible for liquid metals when $Da \geqslant 5 \times 10^{-3}$.

Fig. 6 shows, for fixed $Da = 5 \times 10^{-2}$ and $Pr = 7$, the value of $\overline{\delta_L^*}$ with Jacob number at different values of S_w and Ra. It demonstrates that the higher Jacob number leads to the higher average thickness of condensate liquid in a porous medium and decreases the variation of $\overline{\delta_L^*}$ between Brinkman and Darcy models as $Ja \leqslant 0.22$. To illustrate the effects of the no-slip condition on $\overline{Nu}$, versus Ja, Fig. 7 is plotted. It can be seen that the value of $\overline{Nu}$ decreases as Ja increases. The higher value of Ja implies the higher value of ΔT leads to the increasing average condensate thickness (see Fig. 6) and the decreasing heat transfer rate. The solid lines in Fig. 7 are the solutions based on DM and BM models without suction effect when $Da = 5 \times 10^{-2}$ and $Pr = 7$. It is worth noting that the value of $\overline{Nu}$ by BM when $Ja = 0.25$

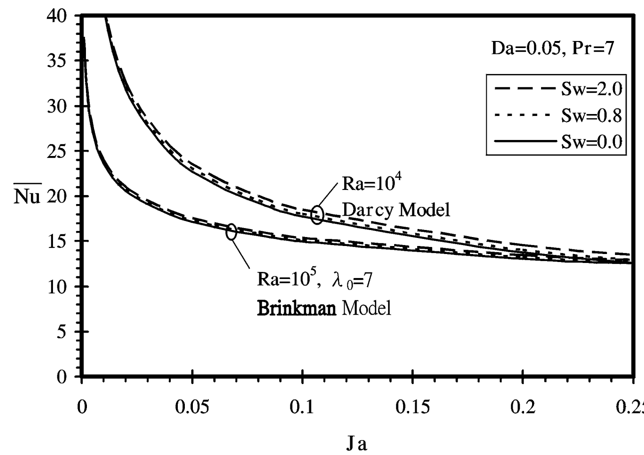

Fig. 7. Variation of the average Nusselt number, $\overline{Nu}$, with Jacob number, Ja, at different values of S_w and Ra for $Da = 5 \times 10^{-2}$, and $Pr = 7$.

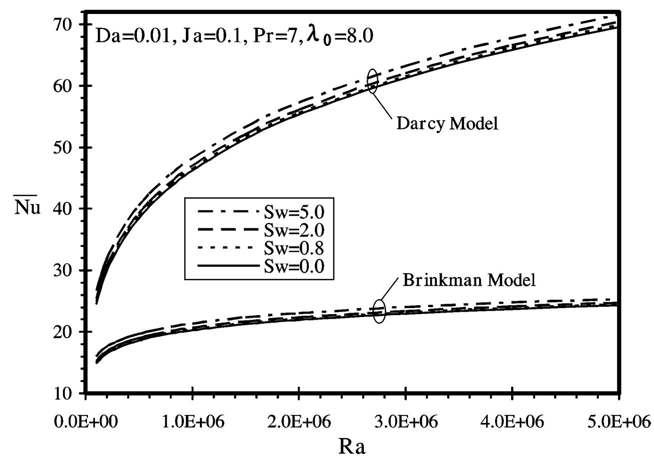

Fig. 8. Variation of $\overline{Nu}$ with Ra at different values of S_w for $Da = 1 \times 10^{-2}$, $Ja = 0.1$, $Pr = 7$ and $\lambda_0 = 8$.

and $Ra = 10^5$ gives the very closed value of $\overline{Nu}$ by DM when $Ja = 0.25$ and $Ra = 10^4$.

The value of $\overline{Nu}$ increases with the increase of Ra at fixed values of Da, Ja, Pr, S_w and λ_0 as shown in Fig. 8. It demonstrates that the higher condensation heat transfer rate is mainly due to the higher convection heat transfer of condensate in a porous medium. From Table 2, it can be seen that $\overline{Nu}$ obtained by using Darcy model is 2.03–3.14 times the $\overline{Nu}$ number by the Brinkman model as $Ra = 5 \times 10^4$–1×10^6 and $S_w = 0$. Accordingly, the viscous boundary effects of the Brinkman model largely reduce the heat transfer rate as the modified Rayleigh number Ra increases.

The variation of average Nusselt number, $\Delta\overline{Nu}$, Eq. (31), and variation percent of average dimensionless film thickness, $\Delta\overline{\delta_L^*}$, Eq. (33), are plotted in Figs. 9 and 10 for various three values of the suction parameter, S_w, respectively. These figures display the comparison of those relations predicted by using both Darcy and Brinkman models. Under fixed values of, Ja, Pr, S_w and λ_0, the value of $\Delta\overline{Nu}$ decreases as values of Ra and the absolute value of $\Delta\overline{\delta_L^*}$ increases. It is seen from Fig. 10 and Table 2 that the higher

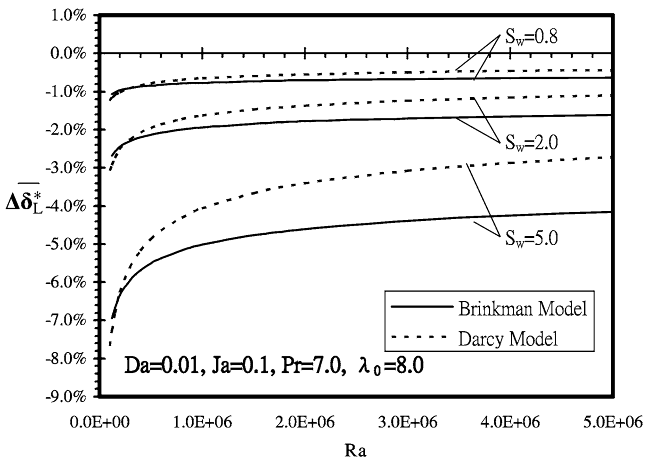

Fig. 9. Variation of $\Delta\overline{\delta^*_L}$ with the modified Rayleigh number, Ra, at different values of S_w for $Da = 1 \times 10^{-2}$, $Ja = 0.1$, and $Pr = 7$.

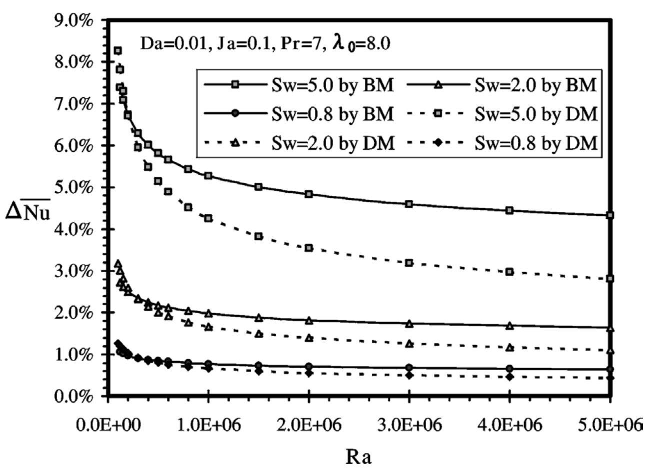

Fig. 10. Variation of $\Delta\overline{Nu}$ with Ra at different values of S_w for $Da = 1 \times 10^{-2}$, $Ja = 0.1$, $Pr = 7$ and $\lambda_0 = 8$.

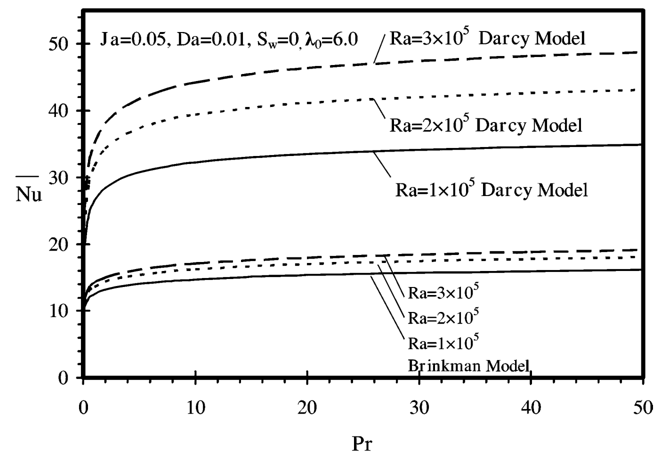

Fig. 11. Variation of the average Nusselt number, $\overline{Nu}$, with Prandtl number, Pr, at different values of Ra for $Ja = 5 \times 10^{-2}$, $Da = 1 \times 10^{-2}$, $S_w = 0$ and $\lambda_0 = 6$.

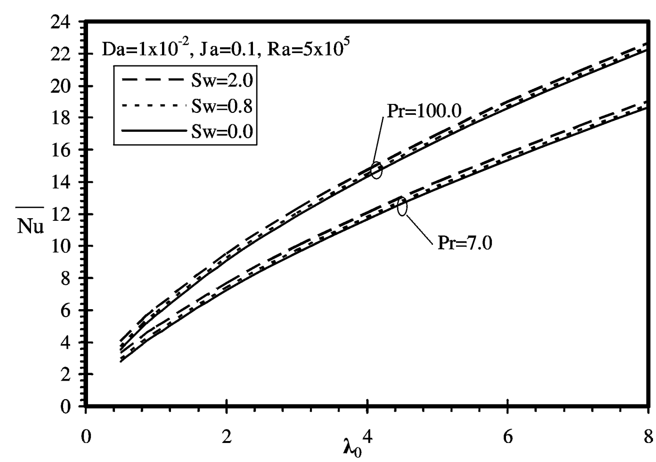

Fig. 12. Variation of the average Nusselt number, $\overline{Nu}$, with permeability number λ_0 at different values of S_w and Pr for $Da = 1 \times 10^{-2}$, $Ja = 0.1$, and $Ra = 5 \times 10^5$ by using BM only.

Table 2
Values of $\overline{Nu}$ as $Da = 10^{-2}$, $Ja = 0.1$, $Pr = 7.0$, for the selected the suction parameter values of S_w by using the Brinkman and Darcy models

$\overline{Nu}$	$Da = 10^{-2}$, $Ja = 0.1$, $Pr = 7.0$			
	BM $\lambda_0 = 5$, $S_w = 0.0$	BM $\lambda_0 = 5$, $S_w = 0.8$	DM $S_w = 0.0$	DM $S_w = 0.8$
$Ra = 5 \times 10^4$	9.918574	10.08297	20.13965	20.44730
$Ra = 1 \times 10^5$	11.00209	11.16402	24.59112	24.89735
$Ra = 3 \times 10^5$	12.74893	12.90843	33.45156	33.75651
$Ra = 5 \times 10^5$	13.57277	13.73162	38.44399	43.01929
$Ra = 8 \times 10^5$	14.34011	14.49855	43.59059	43.89543
$Ra = 1 \times 10^6$	14.70849	14.86679	46.23267	46.53762

suction effect ($S_w > 0$) rapidly increases the convection heat transfer rate as $Ra \leqslant 10^5$. As Ra is lower than 10^4, then the value of $\Delta\overline{Nu}$ for Darcy model is larger than for Brinkman model and the absolute value of $\Delta\overline{\delta^*_L}$ as well. It is due to the predicted value of film thickness by using Darcy model is thinner than by using Brinkman model.

Fig. 11 represents the variation of $\overline{Nu}$ with Pr for fixed $Da = 1 \times 10^{-2}$, $Ja = 5 \times 10^{-2}$, $S_w = 0$ and $\lambda_0 = 6$ at different values of Ra. It demonstrates that the value of $\overline{Nu}$ increases as Pr increases. The value of the permeability parameter λ_0 depends upon the variation of the porosity and permeability of a porous medium. In order to show the variation of λ_0 on the condensation characteristics, Fig. 12 displays the effect of Pr on the dimensionless average heat transfer rate $\overline{Nu}$ vs. permeability parameter, λ_0, at $Da = 0.01$, $Ja = 0.1$, and $Ra = 5 \times 10^5$. It can be seen that $\overline{Nu}$ strictly increases with the increase of the value of λ_0 at fixed values of Da, Ja, Pr and Ra. This can be interpreted that the higher condensation heat transfer rate is mainly due to the higher porosity of the porous medium. This result can be also explained from the fact that the presence of the higher porosity makes much more space for x-directional flow. This implies that the porosity plays a very important role for condensation heat transfer rate in a porous medium. Accordingly, if we have a larger area plate with suction effect, and with a porous

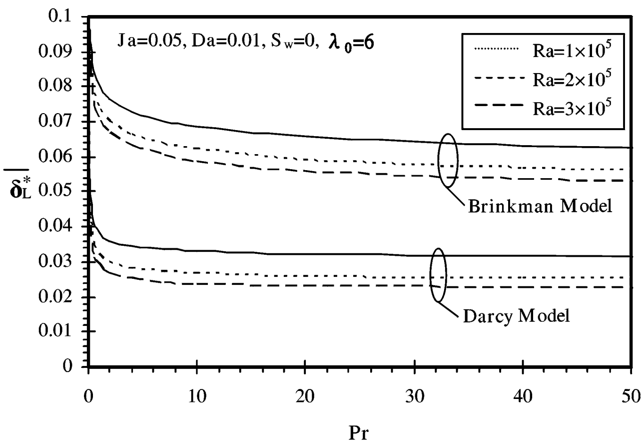

Fig. 13. Variation of the average dimensionless film thickness, $\overline{\delta_L^*}$, with Prandtl number, Pr, at different values of Ra for $Ja = 0.05$, $Da = 0.01$, $S_w = 0$ and $\lambda_0 = 6$.

medium which is higher permeability and porosity, then this can be an effective method to increase condensation heat transfer rate. It is apparent from Fig. 13, which the lower values of the Prandtl number, the greater values of $\overline{\delta_L^*}$ are procured for a fixed value of Ra. It can be demonstrated that Pr represents the relative importance of momentum and energy transport by the diffusion process in a porous medium. The physical significance of the higher Prandtl number, for oils, $Pr \gg 1$, is associated with the larger momentum transport by the diffusion process and is due to the thinner condensation film thickness. Besides, let us consider the case when $Pr \ll 1$, found in liquid metals, which have high thermal conductivity but low viscosity, so that the energy diffusion is much greater than the momentum diffusion. Consequently, as the Prandtl numbers are lower than unity, it is found that the variation of average Nusselt number depends strongly on the values of Ra using the Darcy model.

4. Conclusions

The two-dimensional finite-size horizontal plate covered with a thick porous medium layer is solved numerically by using the fourth-order Runge–Kutta scheme and shooting method. The accuracy of the absolute error 10^{-13} is used to get solutions. The non-dimensional central thickness at the plate decreases as the values of Da, Pr and λ_0 increase. The absolute value of $|\Delta\overline{Nu}|$ is small for the smaller value of S_w (i.e. $S_w \leqslant 0.8$) but it is larger for the smaller Ra (i.e. $Ra \leqslant 10^5$). With fixed the values of Ja, Pr, Ra, and S_w, the influence of λ_0 is more significant than the influence of Da for condensation heat transfer rate as $Da \geqslant 5 \times 10^{-2}$. It is shown that the viscous effect plays an important role for the convection heat transfer in a porous medium as the permeability of a porous medium is very high, so that the Brinkman model is valid for this case. But the values of $\overline{Nu}$ using Darcy model is very close compared with the values of $\overline{Nu}$ using Brinkman model when Ja is larger. In addition, it rapidly reduces the value of $\overline{Nu}$ for oils, $Pr \gg 1$, as the higher Da and Ra, and the lower Ja are specified.

Acknowledgement

The authors expressed a sincere appreciation to the support of the National Science Council, Taiwan, ROC under the grant no. NSC-93-2212-E-269-007.

Appendix A

$$\eta\frac{\mathrm{d}}{\mathrm{d}x^*}\left[\eta\frac{\mathrm{d}\eta}{\mathrm{d}x^*}\right] = -\frac{Ja}{Da\,Ra} \tag{A.1}$$

If we set $t = \eta^2$, $\gamma = 2\eta\eta' = \mathrm{d}t/\mathrm{d}x^*$ and $\mathrm{d}/\mathrm{d}x^* = \gamma \cdot \mathrm{d}/\mathrm{d}t$, Eq. (A.1) becomes

$$\gamma \cdot \mathrm{d}\gamma = -2Ja/(Da\,Ra) \cdot \mathrm{d}t/t^{1/2} \tag{A.2}$$

This is easily done by integrating each side of the above Eq. (A.2), then by using its boundary condition, yielding

$$\gamma = -2\left(\delta_0^* - t^{1/2}\right)^{1/2}\left[2Ja/(Da\,Ra)\right]^{1/2} = 2\eta \cdot \mathrm{d}\eta/\mathrm{d}x^*$$

or

$$\mathrm{d}\eta/\mathrm{d}x^* = -\left(\delta_0^* - \eta\right)^{1/2}\left[2Ja/(Da\,Ra)\right]^{1/2}/\eta \tag{A.3}$$

and the value of $\mathrm{d}\eta/\mathrm{d}x^*$ at $x^* = 1$ can be obtained from Eq. (A.3)

$$\mathrm{d}\eta/\mathrm{d}x^* = -\left[2Ja\left(\delta_0^* - \delta_c^*\right)/(Da\,Ra)\right]^{1/2}/\delta_c^* \tag{A.4}$$

Hence, rearranging Eq. (A.3) and integrating each side of Eq. (A.3) with its boundary condition, we have

$$\begin{aligned}&\left[2Ja/(Da\,Ra)\right]^{1/2}x^*\\&\quad = \delta_0^{*\,3/2}\left(1 - \eta/\delta_0^*\right)^{1/2}\left[4/3 + 2\eta/\left(3\delta_0^*\right)\right]\end{aligned}$$

and thus

$$\left(1 - \eta/\delta_0^*\right)\left(2 + \eta/\delta_0^*\right)^2 = \left[9Ja/\left(2Da\,Ra\,\delta_0^{*3}\right)\right]x^{*2} \tag{A.5}$$

If we let $x^* = 1$ and $\eta = \delta_c^*$, then rewrite Eq. (A.4), and we get

$$\delta_0^* = \left\{9Ja/\left[2Da\,Ra\left(1 - \delta_c^*/\delta_0^*\right)\left(2 + \delta_c^*/\delta_0^*\right)^2\right]\right\}^{1/3} \tag{A.6}$$

From the Eqs. (21b) and (A.4), we have

$$\left[Pr\,\delta_c^*/\left(Da^2 Ra\right)\right]^{1/2} = \left[2Ja\left(\delta_0^* - \delta_c^*\right)/(Da\,Ra)\right]^{1/2}/\delta_c^*$$

and try to rearrange the above equation as

$$\delta_0^* = \left\{2Da\,Ja\left(1 - \delta_c^*/\delta_0^*\right)/\left[Pr\left(\delta_c^*/\delta_0^*\right)^3\right]\right\}^{1/2} \tag{A.7}$$

Substituting Eq. (A.6) into Eq. (A.7), we finally obtain

$$\begin{aligned}&\left(1 - \delta_c^*/\delta_0^*\right)^5\left(2 + \delta_c^*/\delta_0^*\right)^4\\&\quad - 81Pr^3\left(\delta_c^*/\delta_0^*\right)^9/\left(32Da^5 Ja\,Ra^2\right) = 0\end{aligned} \tag{A.8}$$

The value of δ_c^*/δ_0^* from Eq. (A.8) is obtained by using the Newton–Raphson scheme, then the value of δ_0^* from

Eq. (A.7) is easily done. In this case, the values of $\overline{Nu}$ and $\overline{\delta_L^*}$ could be developed as in the following equations

$$\overline{Nu} = \int_0^1 \frac{1}{\eta(x^*)} \mathrm{d}x^* = -\int_{\delta_0^*}^{\delta_c^*} \frac{(0.5Da\,Ra/Ja)^{1/2}}{(\delta_0^* - \eta)^{1/2}} \mathrm{d}\eta$$

$$= \left[\frac{2\delta_0^* Da\,Ra}{Ja}\left(1 - \delta_c^*/\delta_0^*\right)\right]^{1/2} \tag{A.9}$$

$$\overline{\delta_L^*} = \int_0^1 \eta(x^*)\,\mathrm{d}x^* = -\int_{\delta_0^*}^{\delta_c^*} \frac{(0.5Da\,Ra/Ja)^{1/2}\eta^2}{(\delta_0^* - \eta)^{1/2}} \mathrm{d}\eta$$

$$= \frac{\delta_0^{*\,5/2}\{0.5[1 - (\delta_c^*/\delta_0^*)]Da\,Ra/Ja\}^{1/2}}{15} \times \left[6\left(\delta_c^*/\delta_0^*\right)^2 + 8\left(\delta_c^*/\delta_0^*\right) + 16\right] \tag{A.10}$$

References

[1] W. Nusselt, Die oberflächen-kondensation des wasserdampfes, Zeitschrift des Vereines Deutsher Ingenieure 60 (1916) 541–569.

[2] W.M. Rohsenow, Heat transfer and temperature distribution in laminar film condensation, Trans. ASME J. Heat Transfer 78 (1956) 1645–1648.

[3] E.M. Sparrow, J.L. Gregg, A boundary-layer treatment of laminar film condensation, Trans. ASME J. Heat Transfer 8 (1959) 13–18.

[4] M.M. Chen, An analytical study of laminar film condensation: Part 1—Flat plates, Trans. ASME J. Heat Transfer 83 (1961) 48–54.

[5] V.E. Denny, A.F. Mills, Nonsimilar solutions for laminar film condensation on a vertical surface, Int. J. Heat Mass Transfer 12 (1969) 965–979.

[6] J.C.Y. Koh, An integral treatment of two-phase boundary layer in film condensation, Trans. ASME J. Heat Transfer 83 (1961) 359–362.

[7] J.C.Y. Koh, E.M. Sparrow, J.P. Hartnett, The two phase boundary layer in laminar film condensation, Int. J. Heat Mass Transfer 2 (1961) 359–362.

[8] S.W. Churchill, Laminar film condensation, Int. J. Heat Mass Transfer 29 (1986) 1219–1226.

[9] F. Méndez, C. Treviño, Film condensation induced by a natural convective flow: Steady-state analysis, Int. J. Heat Mass Transfer 40 (1997) 1279–1289.

[10] P. Cheng, Film condensation along an inclined surface in a homogeneous porous medium, Int. J. Heat Mass Transfer 24 (1981) 983–990.

[11] K.C. Jain, S.G. Bankoff, Laminar film condensation on a porous vertical with uniform suction velocity, Trans. ASME J. Heat Transfer 86 (1964) 481–489.

[12] N.A. Frankel, S.G. Bankoff, Laminar film condensation on a porous horizontal tube with uniform suction velocity, Trans. ASME J. Heat Transfer 89 (1967) 95–102.

[13] J.W. Yang, Effect of uniform suction on laminar film condensation on a porous vertical wall, Trans. ASME J. Heat Transfer 92 (1970) 252–256.

[14] C.Y. Liu, K.A.R. Ismail, C.D. Ebinuma, Film condensation with lateral mass flux about a body of arbitrary shape in a homogeneous porous medium, Int. Comm. Heat Mass Transfer 11 (1984) 377–384.

[15] C.D. Ebinuma, C.Y. Liu, Film condensation over a permeable non-isothermal body of arbitrary shape in a homogeneous porous medium, Int. Comm. Heat Mass Transfer 11 (1984) 377–384.

[16] I. Pop, D.B. Ingham, Flow past a sphere embedded in a porous medium based on the Brinkman model, Int. Comm. Heat Mass Transfer 23 (1996) 865–874.

[17] M.A. Al-Nimr, M.K. Alkam, Film condensation on a vertical plate imbedded in a homogeneous porous medium, Appl. Energy 56 (1997) 47–57.

[18] M.I. Char, J.D. Lin, H.T. Chen, Conjugate mixed convection laminar non-Darcy film condensation along a vertical plate in a homogeneous porous medium, Int. J. Engng. Sci. 39 (2001) 897–912.

[19] V.D. Popov, Heat transfer during vapor condensation on a horizontal surface, Trudy Kiew. Tecknol. Inst. Pishch. Prom. 11 (1951) 87–97.

[20] S.A. Yang, C.K. Chen, Laminar film condensation on a finite-size horizontal plate with suction at the wall, Appl. Math. Modeling 16 (1992) 325–329.

[21] Y.T. Yang, C.K. Chen, P.T. Hsu, Laminar film condensation on a finite-size horizontal wavy disk, Appl. Math. Modeling 21 (1997) 139–144.

[22] B.A. Bakhmeteff, Hydraulics of Open Channels, McGraw-Hill, New York, 1932, pp. 39–41.

[23] S.-C. Wang, Y.-T. Yang, C.-K. Chen, Effect of uniform suction on laminar filmwise condensation on a finite-size horizontal flat surface in a porous medium, Int. J. Heat Mass Transfer 46 (2003) 4003–4011.

[24] S. Ergun, Fluid flow through packed columns, Chem. Engng. Pro. 48 (1952) 89–94.

[25] D.A. Hield, A. Bejan, Convection in Porous Media, second ed., Springer, New York, 1999.

[26] V.S. Arpaci, P.S. Larsen, Convection Heat Transfer, Prentice-Hall, London, 1984, pp. 277–286.

[27] A. Bejan, Convection Heat Transfer, Wiley, Singapore, 1984, pp. 424–434.